J|A|C|S ARTICLES

Published on Web 01/30/2009

Self-assembly of Collagen Peptides into Microflorettes via Metal Coordination

Marcos M. Pires and Jean Chmielewski*

Department of Chemistry, Purdue University, 560 Oval Drive, West Lafayette, Indiana 47907-2084

Received November 12, 2008; E-mail: chml@purdue.edu

Abstract: The self-assembly of synthetic biomaterials, such as collagen peptides, can be harnessed for a range of biomedical applications. In an effort to obtain collagen-based macromolecular assemblies with temporal control, we designed a system that assembled only in the presence of external stimuli. We report a collagen triple helical peptide that is modified with a His_2 moiety on its C-terminus and a nitrilotriacetic acid unit on its N-terminus that rapidly and reversibly assembles in the presence of metal ions. Dynamic light scattering and turbidity experiments confirmed the presence of higher order aggregates in solution upon the introduction of Zn^{2+}, Cu^{2+}, Ni^{2+}, and Co^{2+}. This assembly process was found to be fully reversible using EDTA as a metal ion chelator. Control peptides that contain only a single ligand-modified terminus were not responsive to the same metal ions, thus demonstrating the requirement of both ligand modifications for peptide assembly. Scanning electron microscopy imaging of the peptide−metal assemblies revealed micrometer-sized florettes in addition to curved, stacked sheets. More detailed analysis of the Zn^{2+}-generated microflorettes showed that the surface of these particles contains ruffled structures with a highly dense surface area. Potential folding intermediates in the formation of the microflorettes were observed at lower temperatures and at early time points in the assembly that are composed of curved layered sheets. Significantly, the assembly process proceeded under mild conditions using neutrally buffered aqueous solution at room temperature. These microscopic structures offer opportunities in many areas, including drug delivery, tissue engineering, and regenerative medicine.

Introduction

The hierarchical assembly of nanoscale building blocks into micrometer-scaled functional materials is a powerful strategy for the design of devices for biomedical applications. For instance, control of scaffold morphology at the nanometer to micrometer scale is one of the current challenges facing successful tissue engineering.[1,2] A range of materials have been used as scaffolds in this context, including biodegradable polymers, and proteins of the extracellular matrix (ECM), such as collagen.[3−5] Problems inherent in the use of natural collagen for tissue engineering include difficulty in the precise control of scaffold morphology and limited ability to introduce chemical diversity. These difficulties could be overcome with collagen peptide building blocks equipped with designed self-assembly signals and specific sites for further functionalization.

Native collagen exists in the ECM as interwoven fibril networks that serve as a scaffold for tissue growth and stability. Collagen-based peptides with repeating units of Pro-Hyp-Gly (Hyp = hydroxyproline) have been shown to adopt a collagen triple helix structure.[6] This core triple helical unit has been used in the formation of collagen-like peptide fibers through the use of electrostatic interactions,[7] $\pi-\pi$ stacking,[8,9] a modified a cysteine knot,[10] native chemical ligation,[11] and radial assembly.[12] Herein we disclose a triple helical collagen peptide, containing distinct metal binding ligands at both termini, that assembles in the presence of transition metal ions to generate collagen-based particles of significant size and distinct shape.

Results and Discussion

The peptide design herein consisted of two salient features: a central collagen-based core composed of nine repeating units of the tripeptide Pro-Hyp-Gly and distinct metal binding ligands at each termini (**NCoH**, Figure 1A). This particular peptide sequence was chosen to ensure the formation of a triple helix with high thermal stability. We envisioned that metal-directed assembly would serve as an appropriate platform to generate

(1) Langer, R.; Vacanti, J. P. *Science* **1993**, *260*, 920–926.
(2) Griffith, L. G.; Naughton, G. *Science* **2002**, *295*, 1009–1014.
(3) Lutolf, M. P.; Hubbell, J. A. *Nat. Biotechnol.* **2005**, *23*, 47–55.
(4) Liu, C.; Czernuszka, J. T. *Mater. Sci. Technol.* **2007**, *23*, 379–391.
(5) Hutmacher, D. W. *J. Biomater. Sci. Polym. Ed.* **2001**, *12*, 107–124.
(6) Persikov, A. V.; Ramshaw, J. A.; Kirkpatrick, A.; Brodsky, B. *Biochemistry* **2000**, *39*, 14960–14967.
(7) Rele, S.; Song, Y.; Apkarian, R. P.; Qu, Z.; Conticello, V. P.; Chaikof, E. L. *J. Am. Chem. Soc.* **2007**, *129*, 14780–14787.
(8) Cejas, M. A.; Kinney, W. A.; Chen, C.; Leo, G. C.; Tounge, B. A.; Vinter, J. G.; Joshi, P. P.; Maryanoff, B. E. *J. Am. Chem. Soc.* **2007**, *129*, 2202–2203.
(9) Cejas, M. A.; Kinney, W. A.; Chen, C.; Vinter, J. G.; Almond, H. R.; Balss, K. M.; Maryanoff, C. A.; Schmidt, U.; Breslav, M.; Mahan, A.; Lacy, E.; Maryanoff, B. E. *Proc. Natl. Acad. Sci. U.S.A.* **2008**, *105*, 8513–8518.
(10) Kotch, F. W.; Raines, R. T. *Proc. Natl. Acad. Sci. U.S.A.* **2006**, *103*, 3028–3033.
(11) Paramonov, S. E.; Gauba, V.; Hartgerink, J. D. *Macromolecules* **2005**, *38*, 7555–7561.
(12) Przybyla, D. E.; Chmielewski, J. *J. Am. Chem. Soc.* **2008**, *130*, 12610–12611.

10.1021/ja8088845 CCC: $40.75

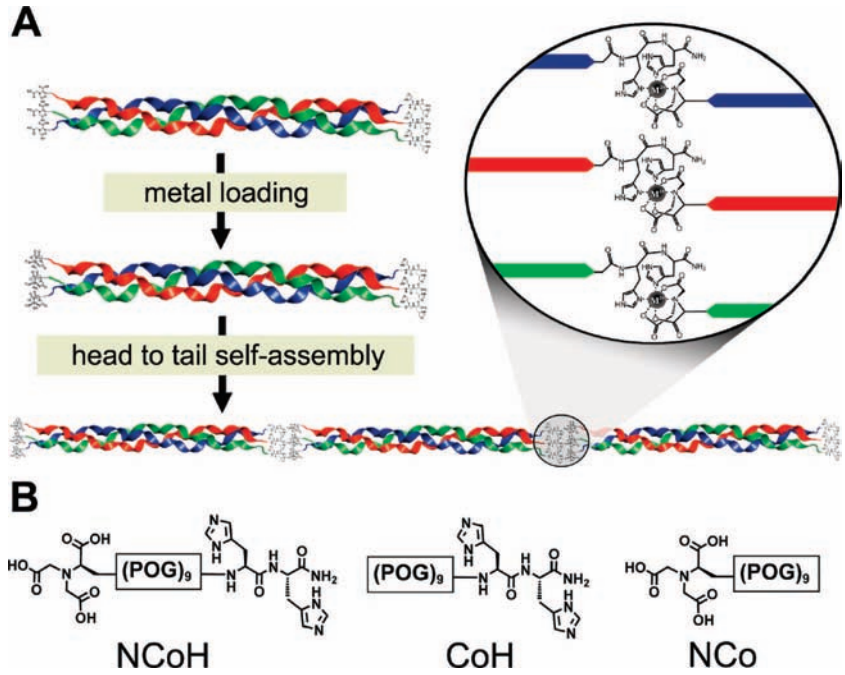

Figure 1. (A) Schematic representation of the design of the **NCoH** peptide and one possible means for assembly. Following the triple helix formation, the addition of metal ions would trigger an initial assembly directed by the NTA and His_2 moieties. (B) Structures of peptides **NCoH**, **CoH**, and **NCo**.

the desired collagen peptide network due to the proven versatility of metal coordination within other polypeptide systems.[13−22] For the metal binding ligands a nitrilotriacetic acid (NTA) unit was installed at the N-terminus and the C-terminus contained a His_2 unit. For this initial design, we included this asymmetry of the metal ligands at the different termini to maintain a continuous register of Pro-Hyp-Gly across the growing assembly (Figure 1A), although we do not rule out possible head-to-head or tail-to-tail assembly as well. Triple helix formation of the individual **NCoH** strands would result in clustering of six histidines at one end of the triple helix and three NTA's at the alternate end—analogous to the NTA/His-tag system frequently used for the purification of proteins. The introduction of the appropriate transition metal would result in directional assembly of individual triple helices. We also designed two control peptides containing either an N-terminal NTA (**NCo**) or a C-terminal His_2 (**CoH**) to probe the role of the combined ligands on metal-promoted assembly (Figure 1B).

All peptides were synthesized using standard Fmoc-based solid phase chemistry. The NTA moiety of **NCoH** and **NCo** was incorporated into the N-terminus via a side chain-linked Fmoc-Glu. Following Fmoc deprotection, the terminal amino group was doubly alkylated with *tert*-butyl bromoacetate to afford the protected NTA unit. Concomitant cleavage from the resin and deprotection of the peptides was accomplished using a TFA cocktail. All peptides were purified to homogeneity using RP-HPLC and characterized with analytical RP-HPLC and MALDI-TOF mass spectroscopy.

Circular dichroism (CD) was used to verify that end modifications did not preclude **NCoH** from forming the expected collagen triple helix and to determine its thermal stability. The CD spectrum of **NCoH** displayed a maximum molar ellipticity at 225 nm that is indicative of the polyproline type II (PPII) helical structure of collagen-like peptides (Figure 2). Cooperative triple helix unfolding was observed for **NCoH** with a melting temperature (T_m) of approximately 50 °C. The decrease in stability of the triple helix of **NCoH** as compared to the analogous peptide $(Pro\text{-}Hyp\text{-}Gly)_9$ ($T_m \sim 67$ °C) is likely a result of electrostatic repulsion at neutral pH due to the NTA termini. Both control peptides (**NCo** and **CoH**) also exhibited a PPII CD profile at 4 °C and each displayed somewhat higher melting temperatures than **NCoH** (58 and 61 °C, respectively). The homotrimerization of individual strands of collagen-like peptides into triple helices is an essential element of our design, as it properly positions and groups the metal binding ligands at each separate termini and, therefore, should allow the propagation of NTA/histidine association between adjoining triple helices.

The effect of different transition metal ions on buffered solutions of **NCoH** was next evaluated. Significant turbidity was observed within the solutions following the addition of metal ions such as Zn(II), Co(II), Ni(II), and Cu(II), but not with Mg(II). Dynamic light scattering (DLS) experiments were used to probe the size of the aggregates in solution. DLS revealed that addition of Zn(II), Co(II), Ni(II), and Cu(II) to **NCoH** each generated particles in solution with a hydrodynamic radius that was greater than 1 μm, whereas addition of Mg(II) to **NCoH** provided a hydrodynamic radius that was similar to that observed for the apo-peptide (Figure 3). The two control peptides, **NCo** and **CoH**, showed no evidence of aggregate

(13) Dublin, S. N.; Conticello, V. P. *J. Am. Chem. Soc.* **2008**, *130*, 49–51.
(14) Burazerovic, S.; Gradinaru, J.; Pierron, J.; Ward, T. R. *Angew. Chem., Int. Ed.* **2007**, *46*, 5510–5514.
(15) Tsurkan, M. V.; Ogawa, M. Y. *Biomacromolecules* **2007**, *8*, 3908–3913.
(16) Cheng, R. P.; Fisher, S. L.; Imperiali, B. *J. Am. Chem. Soc.* **1996**, *118*, 11349–11356.
(17) Koide, T.; Yuguchi, M.; Kawakita, M.; Konno, H. *J. Am. Chem. Soc.* **2002**, *124*, 9388–9389.
(18) Ringler, P.; Schulz, G. E. *Science* **2003**, *302*, 106–109.
(19) Schulze, K.; Mulder, A.; Tinazli, A.; Tampe, R. *Angew. Chem., Int. Ed.* **2006**, *45*, 5702–5705.
(20) Razkin, J.; Nilsson, H.; Baltzer, L. *J. Am. Chem. Soc.* **2007**, *129*, 14752–14758.
(21) DeGrado, W. G.; Summa, C. M.; Pavone, V.; Nastri, F.; Lombardi, A *Annu. Rev. Biochem.* **1999**, *68*, 779–819.
(22) Khurana, R.; Uversky, V. N.; Nielsen, L. A.; Fink, L. *J. Biol. Chem.* **2001**, *276*, 22715–22721.

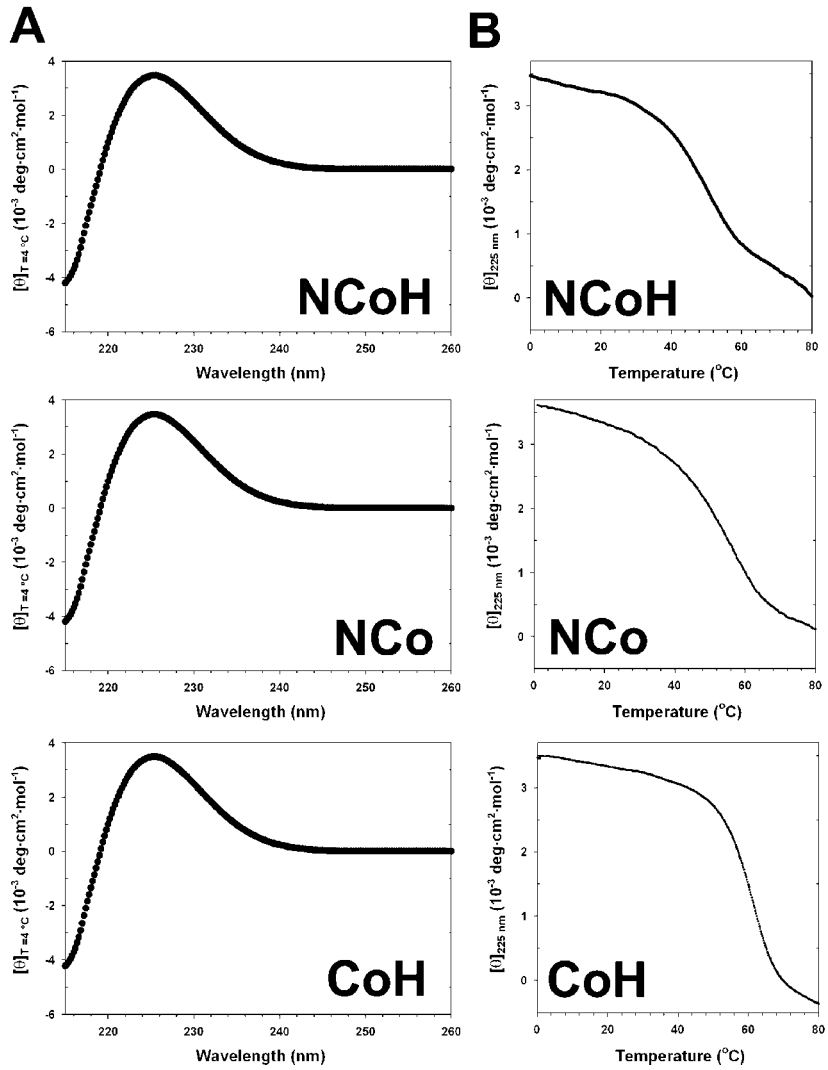

Figure 2. Circular dichroism spectroscopy analysis of **NCoH**, **NCo**, and **CoH**. (A) CD spectroscopy of the specified peptides (500 μM) were measured at 4 °C in 20 mM MOPS buffer, pH 7.4. (B) Thermal denaturation of the specified peptide triple helices was monitored at 225 nm between 0 and 80 °C.

formation by DLS with Cu(II) (data now shown), thereby establishing that triple helices containing either NTA units or His residues at a single termini are not sufficient for the formation of aggregates in solution.

If metal coordination is an intrinsic component of the aggregates, it may be possible to sequester the metal ions with externally added ligands, leading to disruption of assembly. We found that addition of an excess of EDTA to a solution of the $ZnCl_2$-generated particles caused a rapid disappearance of solution turbidity (Figure 4A,B). Full reversibility was observed after addition of the EDTA; reintroduction of metal ions to this same solution yielded a turbid solution once again and this cycle could be repeated. DLS experiments after the addition of EDTA to the $ZnCl_2$-generated particles provided data that was consistent with the metal-free **NCoH** triple helical peptide (Figure 4C). Electron-dispersive X-ray (EDX) analysis confirmed the presence of Zn(II) and Cu(II) ions in the **NCoH**-based particles (see Supporting Information). These data together indicate that the metal ion is a key mediator in the formation of the collagen peptide assemblies.

It became apparent from our experiments that the relative molar ratio between **NCoH** and the metal ion had a significant effect on the assembly process. To investigate this further, **NCoH** was incubated with various ratios of $ZnCl_2$ (Figure 5). Scanning electron microscopy (SEM) analysis revealed that the structural morphology was strongly dependent on the amount of metal ions in solution. For instance, when 0.4 equiv of $ZnCl_2$ was added to **NCoH**, micrometer-sized spherical particles were observed that resembled floretttes (Figure 5B). When the $ZnCl_2$ ratio was halved from this amount (to 0.2 equiv), we observed the formation of open curved tubes composed of what appears to be layered sheets (Figure 5A). Structures formed from increased ratios of $ZnCl_2$ to peptide (0.6 and 0.8 equiv) also deviated from spheres, with the former displaying "C-type" structures (Figure 5C) and the latter showing irregularly shaped flakes (Figure 5D). The addition of an equimolar amount of metal ions as compared to that of **NCoH** resulted in much smaller and finer structures (Figure 5E).

Having established that the addition of metal ions causes higher order aggregates to form with **NCoH**, we were intrigued about the possibility that other transition metal ions might also generate spherical particles as found with $ZnCl_2$(Figure 6C). SEM images of solutions composed of **NCoH** (1 mM) and $CuCl_2$ (400 μM) confirmed that the aggregates that formed in solution were also spherical in nature (Figure 6A). Closer examination by SEM demonstrated that these particles were also

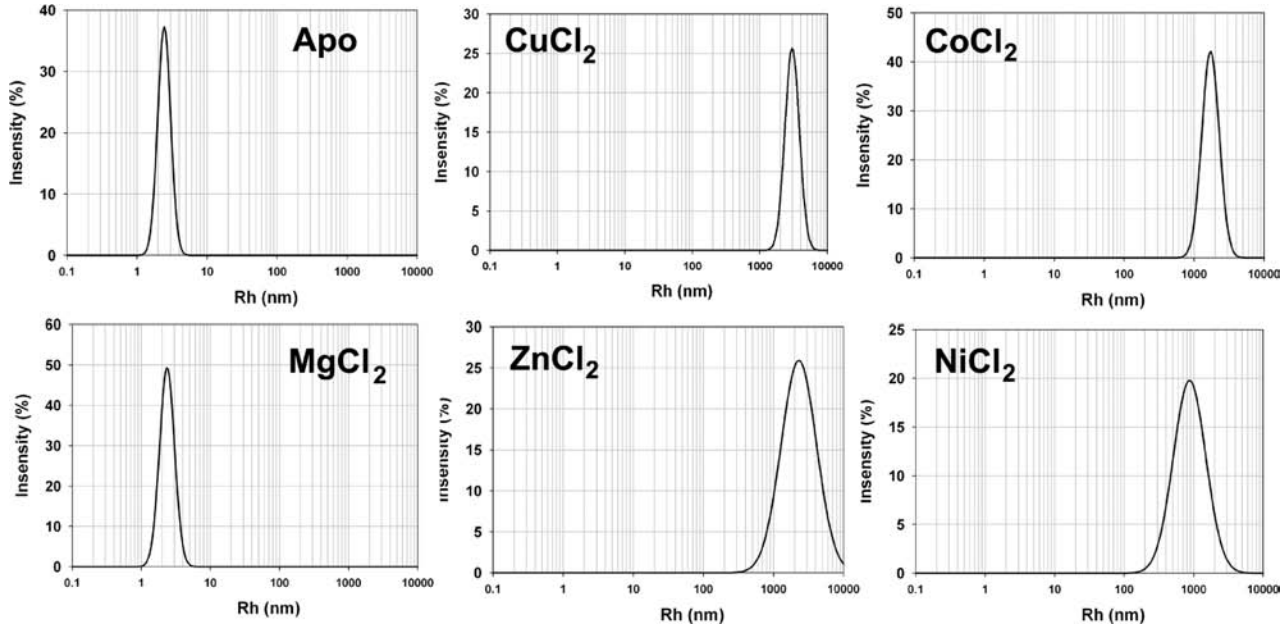

Figure 3. Dynamic light scattering analysis of a metal screen using the **NCoH** peptide. Hydrodynamic radius measurements were obtained using 200 μM of peptide with 100 μM of specified metal ion in 20 mM MOPS (pH 7.4).

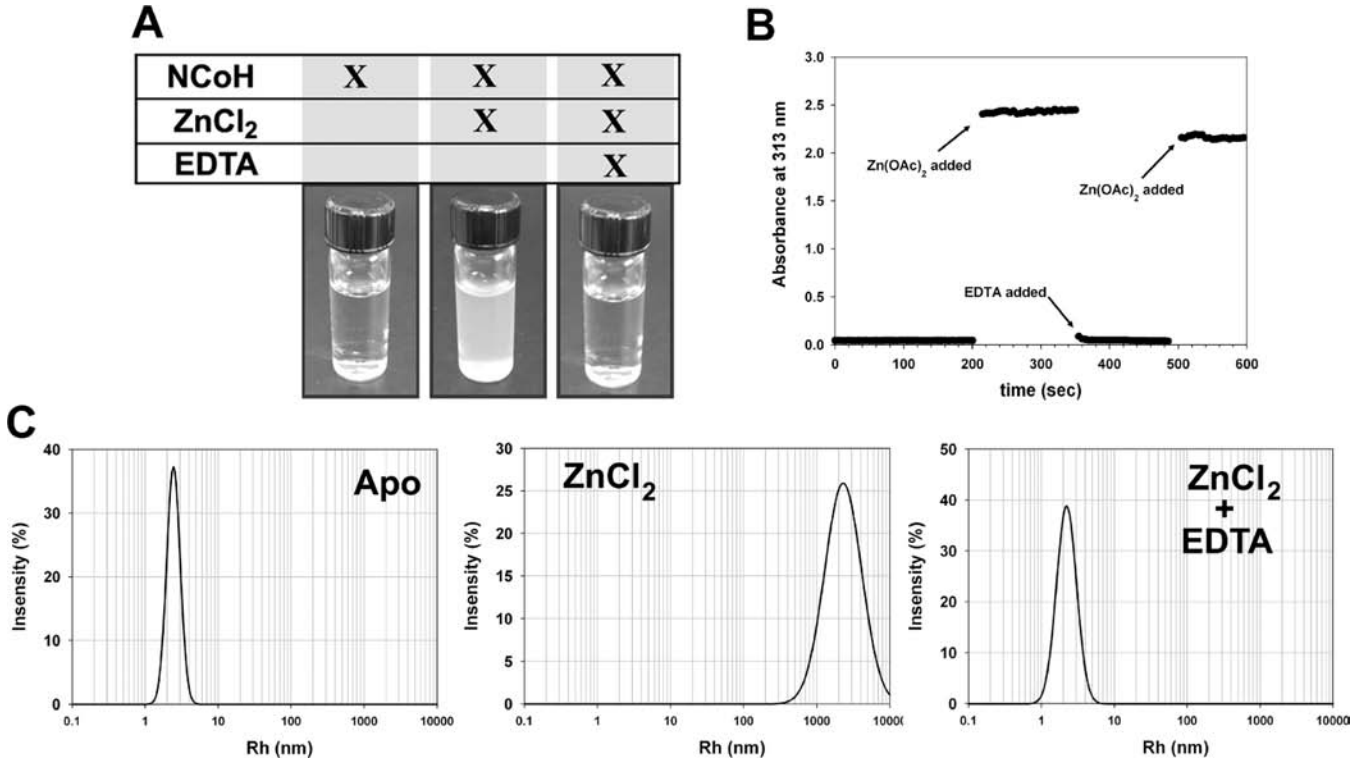

Figure 4. Reversibility of solution turbidity and particle formation. (A) Visualization of solution turbidity containing **NCoH** (250 μM) in 20 mM MOPS, pH 7.4, and 1 mM $Zn(OAc)_2$. The addition of EDTA (10 mM final concentration) causes the disappearance of the turbidity. (B) Solution turbidity was monitored by measuring optical intensity at 313 nm for the above solution of **NCoH** and $Zn(OAc)_2$. At the specified time intervals, EDTA was added (10 mM final concentration), followed by further addition of $Zn(OAc)_2$ (final concentration 3 mM). (C) DLS analysis of chelation competition experiments using the **NCoH** peptide. Hydrodynamic radius measurements were obtained using 200 μM of peptide with 100 μM of $ZnCl_2$ in 20 mM MOPS (pH 7.4) followed by the addition of EDTA (10 mM final concentration).

not smooth, but resembled micrometer-sized florettes (Figure 6B). Treatment of **NCoH** with $CoCl_2$ (400 μM) followed by SEM imaging (Figure 6D) also demonstrated the formation of microflorettes. Although the overall shape of these structures was similar, there were reproducible variations in size with the different metal ions. For instance, Zn(II) ions generated the largest florettes, with many reaching 10−15 μm in diameter. An interesting finding was that **NCoH** assembled in the presence of $NiCl_2$ resulted in a completely different aggregate morphology. Imaging by atomic force microscopy (AFM) showed that the assembled structures were much smaller than those found with other metal ions (Figure 6E). Examination of the AFM

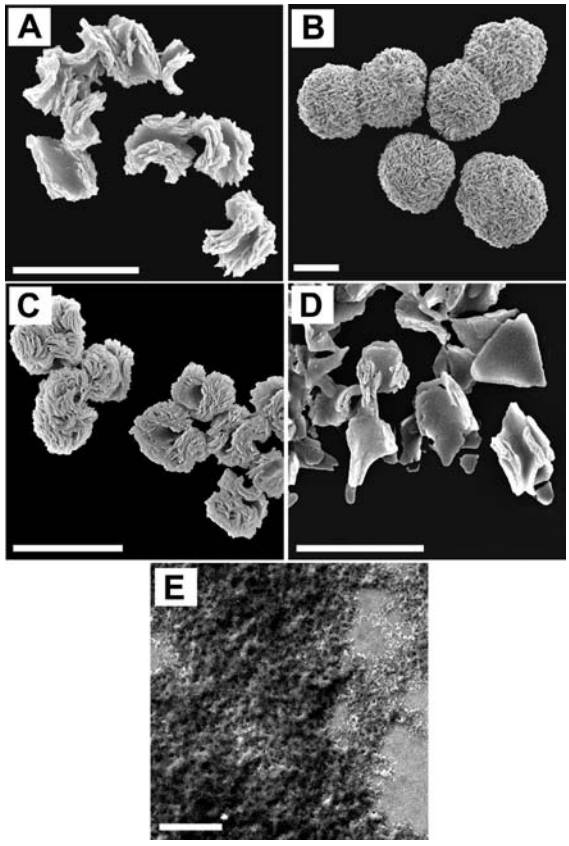

Figure 5. Effect of metal ion concentration on particle morphology. Scanning electron microscopy images of **NCoH** peptide (1 mM) with varying concentrations of $ZnCl_2$: (A) 200 μM $ZnCl_2$; (B) 400 μM $ZnCl_2$; (C) 600 μM $ZnCl_2$; (D) 800 μM $ZnCl_2$; (E) 1 mM $ZnCl_2$. Scale bar = 5 μm.

image revealed that the material is composed of interconnected and irregularly shaped nanosized spheres (50−250 nm).

In an effort to more closely examine the surface of the microflorettes, we obtained higher resolution images of the Zn(II)-based particles (Figure 7A). A densely packed arrangement of individual, ruffled segments on the exterior of the particles was observed with a thickness of the surface-exposed segments of approximately 150 nm. The ruffled surface of the particles may ultimately endow particularly advantageous physical and biophysical properties to these particles simply due to the extended surface area generated by the observed protrusions. To probe the nature of the interior of the particles, Zn(II)-based microflorettes were treated with the fluorescent collagen-binding dye Congo red.[22] Fluorescence microscopy confirmed that Congo red became associated with the particles (Figure 7B). Confocal microscopy was used to image the interior of the particles and demonstrated that the microflorettes were stained throughout with Congo red (Figure 7C), confirming the presence of collagen-like material throughout the interior of the microflorettes.

Our initial conception of metal-promoted assembly with **NCoH** was a linear assembly process (Figure 1). It was quite interesting to us then that this linear design resulted in florette-shaped particles. In an attempt to understand the mechanism of the formation of these structures, we performed the Zn(II)-promoted assembly experiment, using the same conditions that had previously produced microflorettes, except at 4 °C to slow down the formation of the structures. The particles that were generated after 24 h were visualized by SEM (Figure 8A).

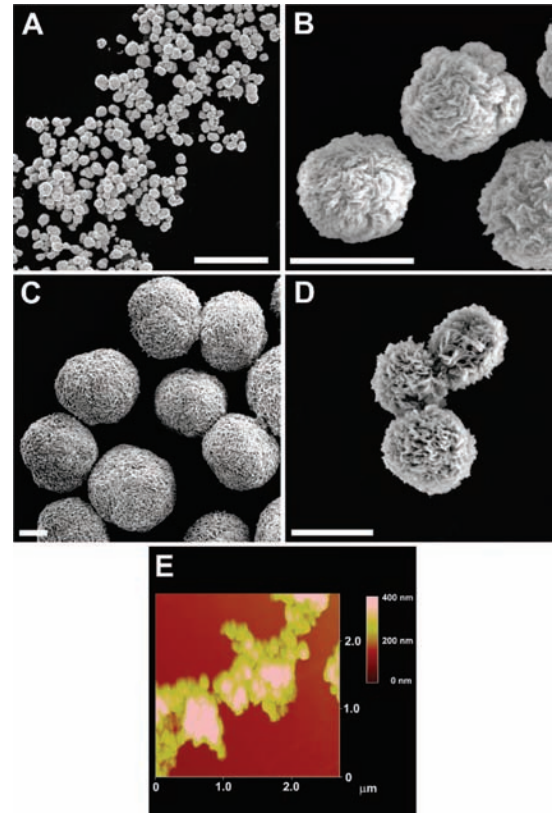

Figure 6. SEM images of **NCoH** peptide (1 mM) with 400 μM $CuCl_2$ (A, scale bar = 100 μm; B, scale bar = 5 μm), 400 μM $ZnCl_2$ (C, scale bar = 5 μm), and 400 μM $CoCl_2$ (D, scale bar = 5 μm). (E) AFM image of **NCoH** peptide (1 mM) with 400 μM $NiCl_2$.

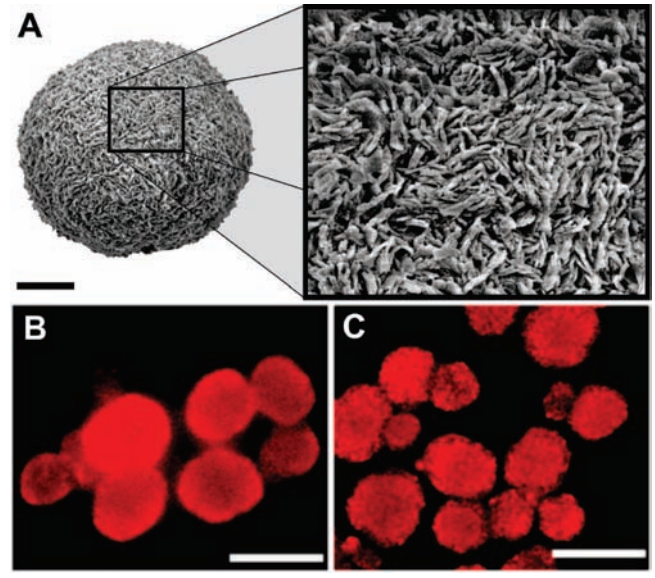

Figure 7. (A) SEM image of the surface of the Zn(II)-based microflorettes (scale bar = 5 μm). Imaging of Zn(II)-based microflorettes treated with Congo red by (B) fluorescence microscopy (scale bar = 20 μm) and (C) confocal microscopy (scale bar = 20 μm).

Interestingly curved layered sheets were observed with a sheet thickness of approximately 60 nm. The addition of Cu(II) to **NCoH** at 4 °C was also monitored after 24 h, and layered sheetlike structures of about the same thickness were also observed (Figure 8B). It is possible that these structures

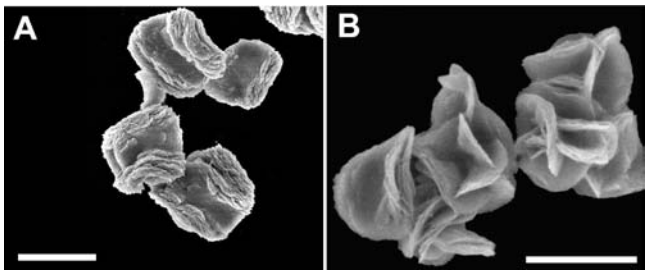

Figure 8. SEM imaging of the **NCoH** peptide (1 mM) at 4 °C with (A) 400 μM $ZnCl_2$ (scale bar = 5 μm) and (B) 400 μM $CuCl_2$ (scale bar = 5 μm).

constitute folding intermediates for the microflorettes and that sheet formation plays a significant role.

To probe the mechanism of growth further, we visualized the structures formed at various time points at room temperature. For instance, the material formed after 5 min with Zn(II) and **NCoH** was found by light microscopy to be composed of about 1 μm particles with an ill-defined background material (Figure 9A). Visualization of this 5 min experiment by SEM demonstrated that the particles after 5 min were composed of curved sheets similar to those observed with Zn(II) at 4 °C (Figure 9B,C). By 30 min, many mature microflorettes had emerged with diameters greater than 5 μm while a significant amount of the background material had disappeared (Figure 9A,B). Clearly, these results demonstrate that the assembly process is nontrivial and appears to consist of multiple intermediates starting as an initial amorphous state, going through curved sheets, before finally equilibrating into highly structured microflorettes. Further AFM imaging of the amorphous background material observed by light microscopy and SEM revealed that this material is composed of interconnected and irregularly shaped nanosized spheres (50−250 nm) (Figure 9D). It is interesting to note that these structures are reminiscent of the nanospheres observed with **NCoH** and Ni(II). It is possible that the Ni(II)-promoted nanospheres (Figure 6E) are trapped in this form, whereas the structure of the Zn(II)-promoted nanospheres may be more dynamic and "evolve" into curved sheet structures followed by the florettes. The insight into how these particles are growing and evolving will serve as starting points in our future attempts to incorporate various elements of chemical diversity into the growing chain of the collagen peptide. Due to the precise temporal control of the assembly process and due to the fact that these collagen-based particles are assembled in a neutral aqueous solution at room temperature, we foresee the utilization of this system for a range of biomedical and drug delivery systems.

Conclusions

Collagen-based peptides that reversibly self-assemble under mild conditions in the presence of metal ions into large and well-ordered structures with tunable shapes and sizes have a myriad of possible uses. The potential exists to incorporate many design parameters, including additional assembly signals for further three-dimensional growth, directed degradation, cell adhesiveness, and release of protein/small molecule therapies, within a single microflorette. The ability to include nanometer to micrometer scale features into such designed biomaterial scaffolds may have significant potential for future biomedical applications.

Experimental Section

Materials. Rink Amide ChemMatrix resin was purchased from Matrix Innovation Inc. (Montreal, Canada). All amino acids and reagents for peptide synthesis were purchased from Novabiochem (La Jolla, CA). AFM wafers were purchased from Ted Pella, Inc. (Tustin, CA). All other chemicals were purchased from Sigma Chemical Co. (St. Louis, MO) and used without further purification.

General Synthesis of Peptides. A 10 mL peptide synthesis flask was loaded with 400 mg (0.20 mmol) of Rink Amide ChemMatrix resin. The resin was initially washed with CH_2Cl_2 (3 × 5 mL) and DMF (3 × 5 mL). Fmoc-protected amino acids (5 equiv, 1.0 mmol) in NMP (5 mL) were added to the reaction flask with HATU (5 equiv, 1.0 mmol) and DIEA (10 equiv, 2.0 mmol), and the flask was agitated for 3 h. The resin was washed with DMF, CH_2Cl_2, MeOH, CH_2Cl_2, and DMF (3 × 5 mL each). Piperidine (20% in NMP, 5 mL) was added to the reaction flask, the flask was agitated for 25 min, and the piperidine solution was drained. The resin was

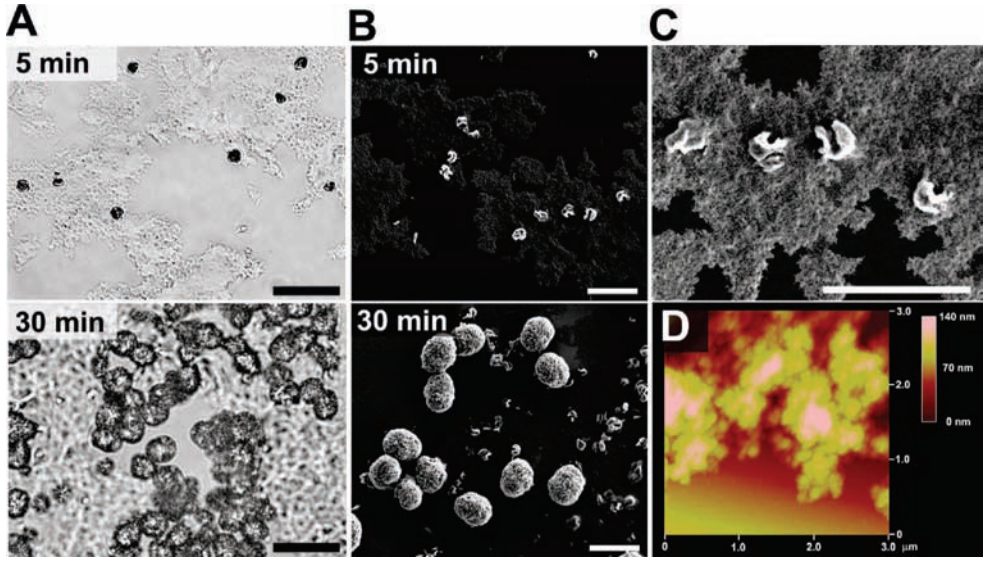

Figure 9. (A) Light microscopy imaging of **NCoH** peptide (1 mM) and 400 μM $ZnCl_2$ at specified time points at room temperature (scale bar = 20 μm). (B and C) SEM imaging of the **NCoH** peptide (1 mM) and 400 μM $ZnCl_2$ at specified time points at room temperature (scale bar = 10 μm). (C) Close-up of the SEM data at 5 min shown in (B) (scale bar = 10 μm). (D) AFM imaging of the background material formed from the **NCoH** peptide (1 mM) and 400 μM $ZnCl_2$ after 5 min at room temperature.

washed with DMF, CH_2Cl_2, and MeOH (2 × 5 mL each). These steps were repeated until all amino acids were coupled to the resin. For the final Fmoc deprotection, piperidine (20% in NMP, 5 mL) was added to the reaction flask; after 25 min the flask was drained. *For peptides containing NTA units*: Fmoc-Glu-O*t*Bu (α-carboxylate protected, 5 equiv, 1.0 mmol) in NMP (5 mL) was added to the reaction flask with HATU (5 equiv, 1.0 mmol) and DIEA (10 equiv, 2.0 mmol), and the flask was agitated for 3 h. The resin was washed with DMF, CH_2Cl_2, MeOH, CH_2Cl_2, and DMF (3 × 5 mL each). Piperidine (20% in NMP, 5 mL) was added to the reaction flask, the flask was agitated for 25 min, and the piperidine solution was drained. The resin was washed with DMF, CH_2Cl_2, and MeOH (2 × 5 mL each). The resin was then treated with *tert*-butyl bromoacetate (5 equiv, 1.0 mmol) and DIEA (10 equiv, 2.0 mmol) in NMP (5 mL), and the flask was agitated for 6 h. *For peptides not containing NTA units*: The peptide was acetylated by adding 8.5% DIEA and 5% Ac_2O in NMP (5 mL) to the flask and agitating it for 1 h. *Cleavage conditions for all peptides:* The resin was washed with DMF, CH_2Cl_2, and MeOH (3 × 5 mL each). A trifluoroacetic acid (TFA) cocktail solution (95% TFA, 2.5% triisopropylsilane, and 2.5% water, 5 mL) was added to the resin, and the mixture was agitated for 2 h. The resulting solution was concentrated in vacuo to remove the TFA. The residue was triturated with cold diethyl ether; the precipitate was collected by centrifugation and dissolved in H_2O. The desired peptide was purified to homogeneity by reverse phase HPLC using a Vydac C18 column with an eluent consisting of solvent A (CH_3CN/0.1% TFA) and solvent B (H_2O/0.1% TFA) with a 60 min gradient consisting of 2−25% A, and a flow rate of 8 mL/min ($\lambda_{214\ nm}$ and $\lambda_{254\ nm}$). HPLC retention times: **NCoH** [21.6 min]; **NCo** [24.7 min]; **CoH** [21.7 min]. Each compound was characterized by MALDI-TOF mass spectrometry. **NCoH** $[M + H]^+$: 2941.37 (calculated), 2941.66 (found). **CoH** $[M + H]^+$: 2736.17 (calculated), 2737.98 (found). **NCo** $[M - H]^-$: 2665.10 (calculated), 2663.29 (found).

Circular Dichorism. CD wavelength scan spectra were recorded on a Jasco circular dichroism spectropolarimeter (Model J810) at 25 °C using a 0.1 cm path length quartz cell. The spectra were averaged over three scans taken from 260 to 210 nm with a resolution of 0.1 nm at a scan rate of 50 nm/min. Thermal stability of peptides was determined by measuring the mean residue ellipticity at 225 nm. Temperature was varied from 0 to 80 °C at 6 °C/h for solutions containing specified peptides (500 μM) in 20 mM MOPS buffer, pH 7.4.

Dynamic Light Scattering. DLS measurements were performed on a DynaPro 99 (Protein Solutions/Wyatt) with laser wavelength of 824 nm. The solutions were measured in 50 μL plastic cuvettes and were placed in a sample holder at 22 °C. The intensity of the size distributions were obtained from the analysis of the correlation functions using a multiple spherical modes algorithm.

Turbidity Experiments. Turbidity experiments were performed by monitoring the absorbance at 313 nm from a solution containing **NCoH** peptide with various metals in 20 mM MOPS buffer, pH 7.4.

Energy-Dispersive X-ray Analysis. Solutions composed of peptides (1 mM) in MOPS buffer (20 mM, pH 7.4) were incubated with desired concentration of the metal ions. Following the assembly of the particles, all solutions were spun at 10000*g* for 3 min and the supernatant was carefully removed. Particles were resuspended in distilled water, and droplets of the sample (5 μL) were air-dried onto carbon tape. Measurements were obtained with an OXFORD INCA 250 electron-dispersive X-ray detector (EDX) operated conjunctly with the FEI NOVA nanoSEM.

Scanning Electron Microscopy Imaging. Scanning electron microscopy images of collagen particles were obtained using a FEI NOVA nanoSEM high-resolution FESEM (FEI Company, Hillsboro Oregon) using the Helix low vacuum detector (0.98T) with operating parameters of 10 kV. Solutions composed of peptides (1 mM) in MOPS buffer (20 mM, pH 7.4) were incubated with desired concentration of the metal ions. Following the assembly of the particles, all solutions were spun at 10000*g* for 3 min and the supernatant was carefully removed. Particles were resuspended in distilled water, and droplets of the sample (5 μL) were air-dried onto glass coverslips. The dried samples were sputter-coated with AuPd (3 min) prior to imaging.

Atomic Force Microscopy Imaging. Samples were prepared as above and droplets of the sample (5 μL) were air-dried onto freshly cleaved mica disks. Collagen particles were imaged in tapping mode on a Multimode AFM with Nanoscope IIIa controller (Veeco) using oxide-sharpened silicon probes having a resonance frequency in the range of 280−320 kHz (MikroMasch-NSC15). The tip−surface interaction was minimized by optimizing the scan set point to the highest possible value.

Fluorescence Microscopy Imaging. For fluorescence microscopy images, particle solutions (25 μL) produced from the combination of **NCoH** peptide (1 mM) with $ZnCl_2$ (400 μM) in 20 mM MOPS buffer at pH 7.4 were incubated with Congo red (100 μM final concentration). All solutions were spun at 10000*g* for 3 min and the supernatant was carefully removed. To the remaining pellet was added 100 μL of 20 mM MOPS buffer at pH 7.4, the solution was vortexed for 20 s, and the Eppendorf tube was once again spun down at 10000*g* for 3 min. The supernatant was carefully removed, and the particles were resuspended in 20 μL of 20 mM MOPS buffer at pH 7.4 and plated onto a glass slide. Images were captured using an Optical Microscope Olympus BX51 equipped with a CCD camera. Congo red was excited using a U-MWG2 filter with excitation of 510−550 nm.

Confocal Microscopy. For confocal microscopy images, particle solutions (25 μL) produced from the combination of **NCoH** peptide (1 mM) with $ZnCl_2$ (400 μM) in 20 mM MOPS buffer at pH 7.4 were incubated with Congo red (100 μM final concentration). All solutions were centrifuged at 10000*g* for 3 min and the supernatant was carefully removed. To the remaining pellet was added 100 μL of 20 mM MOPS buffer at pH 7.4, the solution was vortexed for 20 s, and the solution was once again centrifuged at 10000*g* for 3 min. The supernatant was carefully removed, and the particles were resuspended in 20 μL of 20 mM MOPS buffer at pH 7.4 and plated onto a glass slide. Images were acquired using a Radiance 2100 MP Rainbow (Bio-Rad, Hemel Hempstead, England) on a TE2000 (Nikon, Tokoyo, Japan) inverted microscope using a 60× oil 1.4 NA lens. Congo red was excited at 543 nm using the green HeNe laser and the fluorescence emission greater than 560 nm in wavelength was collected.

Acknowledgment. We thank D. Przybyla for helpful discussions and financial support from the NSF (Grant 0078923-CHE).

Supporting Information Available: Supplemental EDX data. This material is available free of charge via the Internet at http://pubs.acs.org.

JA8088845